Molecular Therapy
Original Article

Optimization of IL13Rα2-Targeted Chimeric Antigen Receptor T Cells for Improved Anti-tumor Efficacy against Glioblastoma

Christine E. Brown,[1] Brenda Aguilar,[1] Renate Starr,[1] Xin Yang,[1] Wen-Chung Chang,[1] Lihong Weng,[1] Brenda Chang,[1] Aniee Sarkissian,[1] Alfonso Brito,[1] James F. Sanchez,[1] Julie R. Ostberg,[1] Massimo D'Apuzzo,[2] Behnam Badie,[3] Michael E. Barish,[4] and Stephen J. Forman[1]

[1]Department of Hematology & Hematopoietic Cell Transplantation, T Cell Therapeutics Research Laboratory, City of Hope Beckman Research Institute and Medical Center, Duarte, CA 91010, USA; [2]Department of Pathology, City of Hope Medical Center, Duarte, CA 91010, USA; [3]Department of Neurosurgery, City of Hope Medical Center, Duarte, CA 91010, USA; [4]Department of Developmental and Stem Cell Biology, City of Hope Beckman Research Institute, Duarte, CA 91010, USA

T cell immunotherapy is emerging as a powerful strategy to treat cancer and may improve outcomes for patients with glioblastoma (GBM). We have developed a chimeric antigen receptor (CAR) T cell immunotherapy targeting IL-13 receptor α2 (IL13Rα2) for the treatment of GBM. Here, we describe the optimization of IL13Rα2-targeted CAR T cells, including the design of a 4-1BB (CD137) co-stimulatory CAR (IL13BBζ) and a manufacturing platform using enriched central memory T cells. Utilizing orthotopic human GBM models with patient-derived tumor sphere lines in NSG mice, we found that IL13BBζ-CAR T cells improved anti-tumor activity and T cell persistence as compared to first-generation IL13ζ-CAR CD8$^+$ T cells that had shown evidence for bioactivity in patients. Investigating the impact of corticosteroids, given their frequent use in the clinical management of GBM, we demonstrate that low-dose dexamethasone does not diminish CAR T cell anti-tumor activity in vivo. Furthermore, we found that local intracranial delivery of CAR T cells elicits superior anti-tumor efficacy as compared to intravenous administration, with intraventricular infusions exhibiting possible benefit over intracranial tumor infusions in a multifocal disease model. Overall, these findings help define parameters for the clinical translation of CAR T cell therapy for the treatment of brain tumors.

INTRODUCTION

Glioblastoma (GBM) is both the most common and most aggressive type of primary malignant brain tumor. While standard-of-care treatment, including surgical resection followed by radiation and adjuvant chemotherapy, may provide short-term benefits,[1] GBM remains nearly uniformly lethal. Treatment failure is commonly due to therapy-resistant invasive malignant cells that are the root of tumor recurrence, and the refractory nature of GBM provides a rationale and motivation for developing novel treatment interventions for this intractable disease.

Adoptive cell therapy using T cells that are genetically modified to express chimeric antigen receptors (CARs) is a promising therapeutic approach that enables large numbers of patient-specific T cells to be rapidly generated, which then direct potent, antigen-specific tumor eradication. The remarkable clinical success observed with CD19-CAR T cells for the treatment of CD19$^+$ B cell malignancies,[2–4] most strikingly in patients with refractory acute lymphoblastic leukemia (ALL),[5] provides optimism that this therapy can improve therapeutic outcomes for patients with other cancers, including brain tumors. Indeed, CD19-CAR T cells have been shown to accumulate in the cerebrospinal fluid (CSF) and reduce the incidence of metastatic leukemic disease in the brain.[6–9] Furthermore, administration of melanoma-specific tumor infiltrating lymphocytes (TIL) has been shown to eliminate a metastatic lesion in the brain.[10] However, the application of CAR T cell therapy for the treatment of brain tumors is still in the early stages of development, with many of the unique parameters specific to the location and biology of this disease still under active investigation.

One challenge for the development of CAR T cell immunotherapy for GBM is the identification of tumor antigens that are broadly expressed on the cell surface and, importantly for safety considerations, are not highly expressed on normal brain or other life-sustaining tissues. An attractive immunotherapeutic target meeting these criteria is IL-13 receptor α2 (IL13Rα2), a monomeric high-affinity interleukin-13 (IL-13) receptor, which is overexpressed by the majority of GBM tumors (>60%) and not expressed at significant levels on normal brain tissue.[11–15] IL13Rα2 expression is closely associated with that of the mesenchymal GBM subtype and is a prognostic indicator of poor

Received 4 May 2017; accepted 1 October 2017;
https://doi.org/10.1016/j.ymthe.2017.10.002.

Correspondence: Christine E. Brown, Hematology & Hematopoietic Cell Transplantation, T Cell Therapeutics Research Laboratory, City of Hope Beckman Research Institute and Medical Center, Duarte, CA 91010, USA.
E-mail: cbrown@coh.org

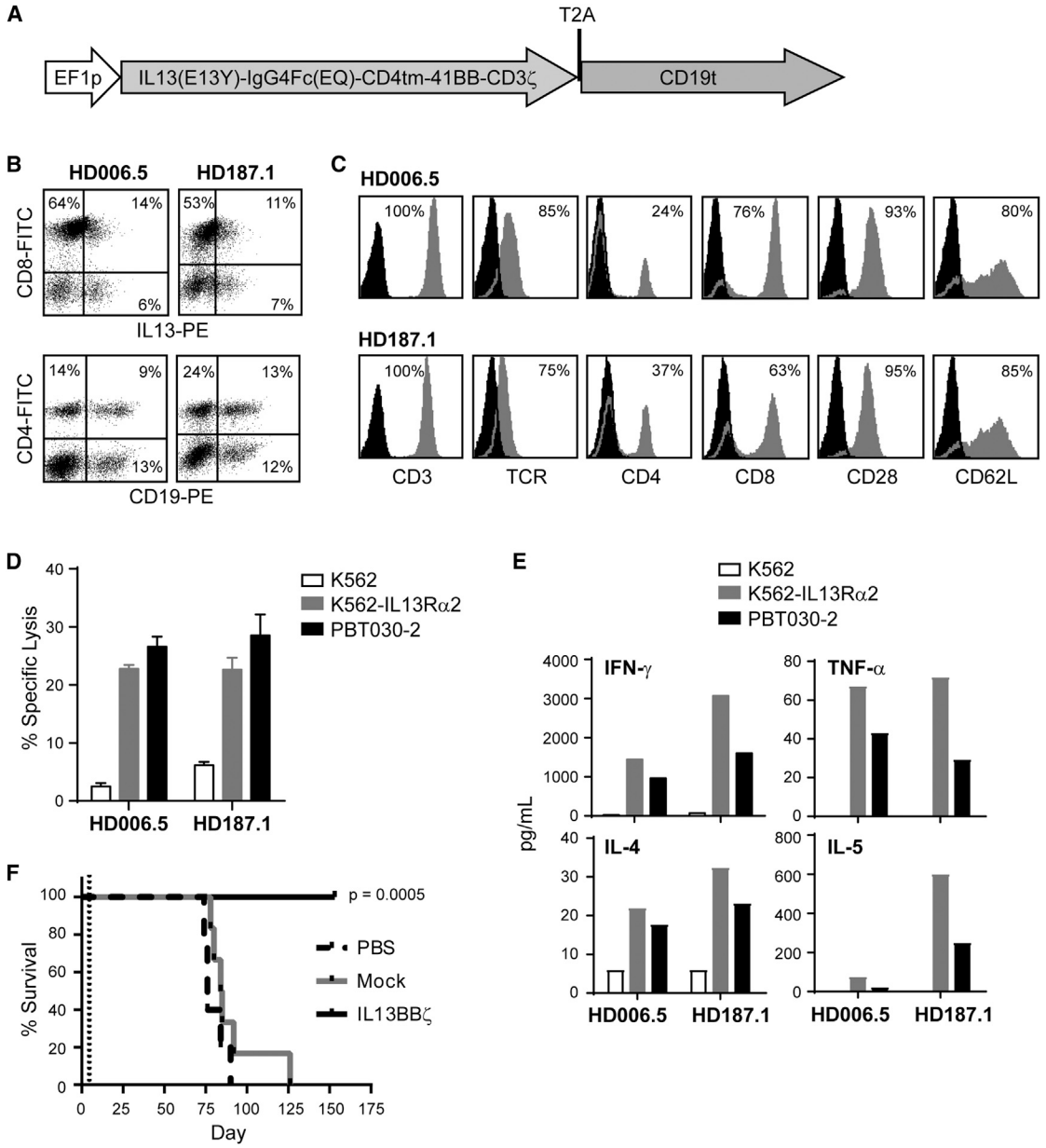

Figure 1. Engineering and Characterization of IL13BBζ T Cells

(A) Diagram of cDNA open reading frame of the 2,670-nucleotide IL13(EQ)BBζ-T2A-CD19t construct, where the EF1 promoter (EF1p) drives transcription of the IL13BBζ CAR (containing the IL13Rα2-selective ligand IL13(E13Y), IgG4Fc(EQ) linker, CD4 transmembrane domain [CD4tm], 4-1BB [CD137] cytoplasmic signaling domain, and CD3ζ cytoplasmic signaling domain sequences), as well as the T2A ribosomal skip and truncated CD19 (CD19t) sequences. (B) IL13BBζ T cells derived from healthy donors HD006.5 and HD187.1 were co-stained with anti-IL13-PE and anti-CD8-FITC (top) or anti-CD19-PE and anti-CD4-FITC (bottom) to detect the proportion of $CD8^+$ and $CD4^+$ cells that express the CAR and CD19t transgenes. Histogram quadrants were drawn based on isotype control staining, and percentages of immunoreactive cells are indicated in each quadrant. (C) HD006.5 and HD187.1 IL13BBζ T cells were stained with fluorochrome-conjugated anti-CD3, TCR, CD4, CD8, CD28, and CD62L (gray histograms). Percentages of immunoreactive cells above isotype controls (black histograms) are indicated in each histogram. (D) HD006.5 and HD187.1 IL13BBζ T cells were used as effectors in a 6 hr ^{51}Cr release assay using a 10:1 effector-to-target (E:T) ratio based on CD19t expression. The IL13Rα2-positive tumor targets were K562 cells engineered to express IL13Rα2 (K562-IL13Rα2) and the primary glioma line PBT030-2; the negative tumor target control was the parental K562 line. Means + SD of triplicate wells are depicted. (E) HD006.5 and HD187.1 IL13(EQ)BBζ T cells were evaluated for antigen-dependent Th1 (e.g., IFN-γ, TNF-α) and Th2 (e.g., IL-4, IL-5) cytokine production following overnight co-culture at a 10:1 E:T ratio (based on CD19t expression) with the same IL13Rα2-positive and negative

(legend continued on next page)

patient survival.[11] This favorable expression profile provides the rationale for continued development of CAR T cells targeting IL13Rα2.[16–20] Our clinical experience with first-generation IL13Rα2-targeted CAR T cells in patients with GBM demonstrated the overall safety and tolerability of this therapeutic approach, with evidence for anti-tumor activity.[21] Here, we describe studies aimed at refining both the CAR T cell product and the clinical parameters for optimally translating this therapy to GBM patients. These studies provided foundation for and helped drive the protocol design of our recently opened phase I clinical trial for GBM (NCT02208362), in which complete remission of recurrent multifocal GBM was observed in a single patient.[22]

RESULTS

Development of Second-Generation IL13Rα2-Targeting CAR T Cells

We have designed a second-generation IL13Rα2-targeted CAR, termed IL13BBζ (Figure 1A), which, similar to our previously described first-generation IL13ζ CAR,[18,19,21] recognizes IL13Rα2 through a membrane-tethered IL-13 ligand, modified at a single site (E13Y).[23] IL13BBζ then also incorporates an optimized IgG4-Fc linker mutated at two sites within the CH2 region (L235E; N297Q) to reduce Fc receptor binding,[24] and the intracellular signaling domain of CD137 (4-1BB) in series with CD3ζ, as the 4-1BB costimulatory sequence has been suggested to prevent anergy and promote persistence of CAR T cells.[25] In addition, our CAR expression cassette includes the T2A ribosome skip sequence[26] followed by a truncated CD19 (CD19t) (Figure 1A), a non-signaling cell surface marker applicable for cell tracking and enrichment. This expression cassette design allows the IL13BBζ CAR and CD19t to be expressed from a single mRNA transcript but translated as two separate proteins that independently traffic to the cell membrane.

For this study, enriched primary human central memory T cells (Tcm) ($CD45RA^-$, $CD62L^+$) were lentivirally transduced to express IL13BBζ and CD19t. We focused on Tcm, as this memory population has been shown to have favorable properties for therapeutic application, including long-term persistence upon adoptive transfer in vivo,[27–29] and our group has developed processes to isolate, genetically modify, and culture CAR^+ Tcm products for clinical investigation.[30] As exemplified by two engineered human T cell lines derived from healthy donors (HD006.5 and HD187.1), lentiviral transduction yields cell surface expression of both the IL13BBζ-CAR and CD19t, confirmed by flow cytometry with anti-IL13 and anti-CD19 antibodies, respectively (Figure 1B). After ex vivo expansion of these CAR T cells for up to 28 days, the products retained expression of central memory markers CD62L and CD28 (Figure 1C).

These Tcm-derived IL13BBζ T cells efficiently recognize and kill $IL13Rα2^+$ target cells. By chromium release assay, both the IL13Rα2-engineered K562 line (K562-IL13Rα2; Figure S1), and the IL13Rα2-expressing PBT030-2 primary glioma line were lysed more than 3-fold over the IL13Rα2-negative parental K562 line (Figure 1D). Overnight co-culture with $IL13Rα2^+$ cells also stimulated the IL13BBζ T cells to secrete cytokines (Figure 1E), whereas minimal secretion was observed upon co-culture with IL13Rα2-negative K562 cells. These engineered IL13BBζ T cells also exhibited strong anti-tumor efficacy in our previously established in vivo xenograft brain tumor model with $IL13Rα2^+$ PBT030-2 cells that had been engineered to express the firefly luciferase (ffLuc) reporter gene.[19] With this $ffLuc^+$ PBT030-2 tumor xenograft model (1×10^5 cells intracranially; 5 days engraftment), NOD.Cg-Prkdcscid Il2rgtm1WjI/SzJ (NSG) mice treated with a single intracranial tumor (ICT) injection of mock-transduced T cells (no CAR expression) exhibited tumor growth and survival similar to that of non-treated controls, while mice treated with the IL13BBζ T cells exhibited significantly improved survival (Figure 1F). The anti-tumor activity of ICT administered IL13BBζ T cells can also be observed in the more aggressive glioma tumor models U251T and PBT103-2-Rα2 (Figure S2).

IL13BBζ T Cells Display IL13Rα2-Selective Effector Activity

There are two receptors that bind the IL-13 cytokine, IL13Rα1 and IL13Rα2. IL13Rα1 is a widely expressed low-affinity receptor that heterodimerizes with IL-4Rα following IL-13 binding to initiate IL-13 immune functions.[31] IL13Rα2 is a high-affinity monomeric receptor, with restricted expression on normal tissue and frequent overexpression in a number of human cancers, including GBM.[13,31] Thus, to evaluate the relative targeting of these two receptors by our IL-13(E13Y)-ligand based CAR, we first tested the ability of plate-bound recombinant human IL13Rα1-Fc and IL13Rα2-Fc to stimulate the IL13BBζ T cells to produce interferon-γ (IFN-γ). When challenged with equivalent recombinant receptor concentrations, IL13BBζ T cells produced much stronger IFN-γ responses to human IL13Rα2-Fc as compared to human IL13Rα1-Fc (3.2-fold higher at receptor concentration 250 ng/mL, $p = 0.000002$ using an unpaired Student's t test; Figure 2A). However, the CAR T cell IFN-γ response to plate bound human IL13Rα1-Fc, though minimal, was still higher than that observed with mock-transduced T cells ($p = 0.0001$ at receptor concentration 250 ng/mL using an unpaired Student's t test; Figure 2A). We went on to examine IL13BBζ T cell responses to human tumor cell targets expressing IL13Rα1 and IL13Rα2. Each of the tumor cell lines expressed similar levels of endogenous IL13Rα1, as exemplified by the fibrosarcoma line HT1080, with relatively lower expression levels detected on the lymphoblastoid cells (both lymphoblastoid cell lines [LCLs] and positive control LCL-OKT3, which expresses the membrane-bound single chain variable fragment [scFv] derived from the CD3 agonist antibody OKT3) (Figure 2B). By contrast, IL13Rα2 was more highly expressed by the GBM tumor line PBT030-2, as

targets as described in (D). (F) Kaplan-Meier survival analysis demonstrating significantly improved survival for mice treated with IL13BBζ T cells as compared to mock-transduced T cells. Primary brain-tumor-derived PBT030-2 cells (1×10^5) were stereotactically implanted into the right forebrain of NSG mice. On day 5 (dotted line), mice (n = 6 per group) received intracranial tumor (ICT) injections of either PBS, 2×10^6 mock-transduced T cells (Mock), or 2×10^6 IL13BBζ T cells (IL13BBζ). $p = 0.0005$ when comparing the IL13BBζ and Mock groups using the log rank (Mantel-Cox) test.

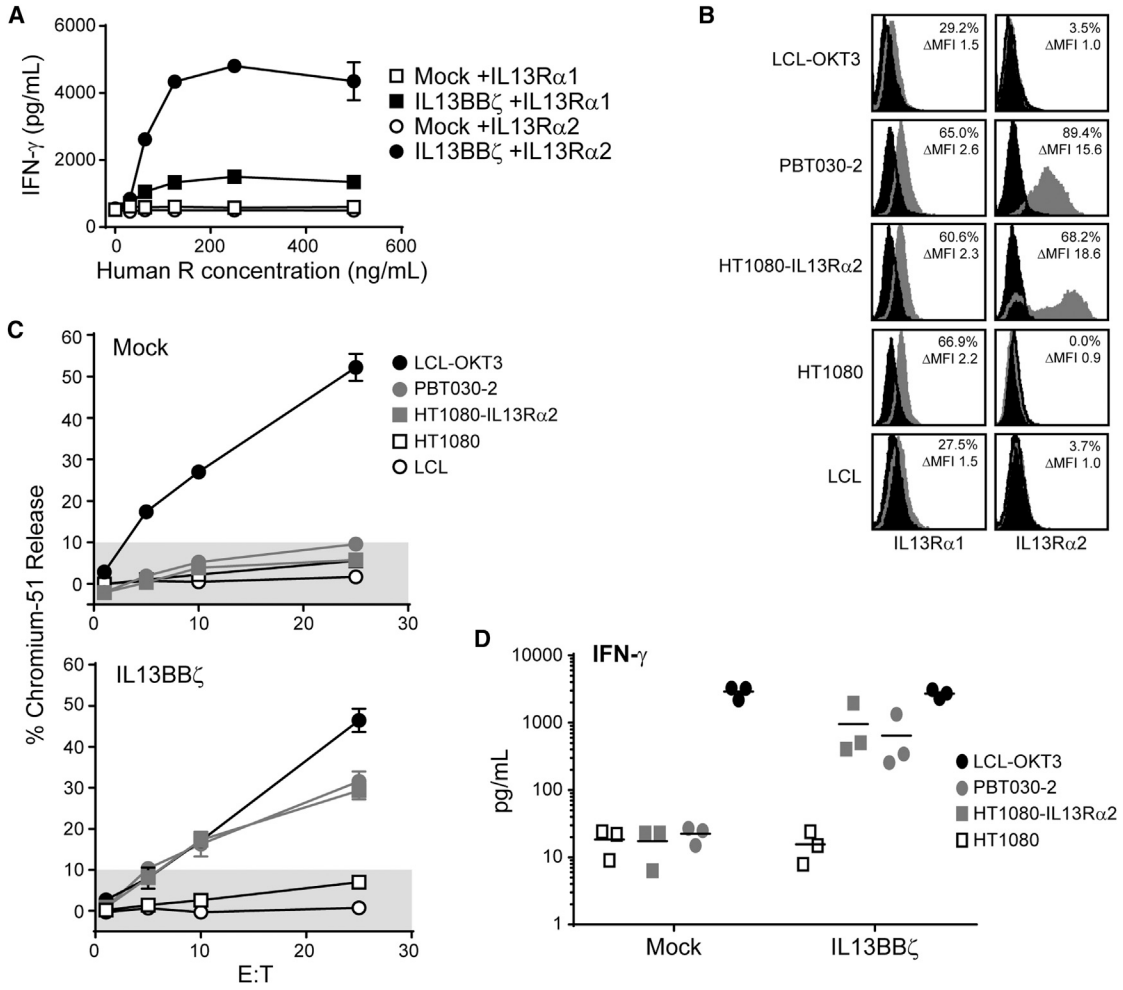

Figure 2. IL13BBζ T Cells Mediate IL13Rα2-Selective In Vitro Function

(A) Mock-transduced T cells (Mock, open symbols) or IL13BBζ T cells (black symbols) were cultured overnight on 96-well plates that had been coated with titrated concentrations of recombinant human IL13Rα1-Fc (squares) or IL13Rα2-Fc (circles). Supernatants were then evaluated for IFN-γ levels by ELISA. Means ± SD of triplicate wells are depicted. Data are representative of experiments done with Tcm derived from three different healthy donors. (B) Flow cytometric analysis of IL13Rα1 and IL13Rα2 on target/stimulator lines. Percentages of viable immunoreactive cells (%) and fold differences in mean fluorescence intensity (ΔMFI) compared to secondary reagent alone (black histograms) are depicted in each histogram. (C) Four-hour ^{51}Cr-release assays were performed with mock-transduced T cells (top) or IL13BBζ T cells (bottom) as effectors and the indicated tumor lines as targets. Percent ^{51}Cr-release (mean ± SD of three wells) at E:T ratios of 1:1, 5:1, 10:1, and 25:1 (based on total cell number) is depicted. Shaded regions of each graph indicate background cytolytic activity as defined by the mock-transduced controls. Data are representative of experiments done with Tcm derived from three different healthy donors. (D) Mock-transduced T cells (Mock) or IL13BBζ T cells from three different healthy donors were stimulated with the same tumor lines as in (C). Stimulation with LCL-OKT3 served as a positive control. IFN-γ levels were measured using Human Cytokine Bead Array, and lines indicate mean values.

well as the engineered HT1080-IL13Rα2, consistent with it often being overexpressed under pathological conditions (Figure 2B).[31] We found that the IL13Rα2-expressing targets PBT030-2 and HT1080-IL13Rα2 were efficiently lysed by the IL13BBζ T cells (Figure 2C) and stimulated cytokine (e.g., IFN-γ) production by the IL13BBζ T cells (Figure 2D; Table S1). Such effector activity against the tumor lines that only express endogenous IL13Rα1 (i.e., LCL, parental HT1080) was never above that observed with mock-transduced Tcm. Taken together, these studies support the IL13Rα2 selectivity of the IL13BBζ T cells.

IL13BBζ T Cells Are More Potent Than a First-Generation CAR T Cell Clone

We sought to directly compare the anti-tumor potency of our optimized second-generation IL13BBζ-CAR T cell product versus our earlier, non-costimulatory, non-Tcm, IL13ζ-CAR-expressing CD8$^+$ T cell clone,[18] as first-generation IL13ζ CD8$^+$ T cell clones have been evaluated in patients, displaying safety and transient anti-tumor activity.[21] For these experiments, we again used the ffLuc$^+$ PBT030-2 tumor xenograft model, where mice treated with a single ICT injection of mock-transduced T cells exhibited tumor growth similar to

that of non-treated controls (Figure 3). Mice treated with a single injection of the IL13ζ $CD8^+$ clone 2D7 exhibited some tumor growth control and improved survival at only the highest (1×10^6) CAR^+ T cell dose. In comparison, a single administration of the IL13BBζ T cells was more efficient at reducing tumor burden, with the lower doses of 0.3×10^6 and 0.1×10^6 CAR^+ T cells being almost as effective as the highest 1×10^6 dose. Indeed, a 0.1×10^6 dose of the IL13BBζ T cells was significantly more effective than even the 1×10^6 dose of the IL13ζ $CD8^+$ clone 2D7 cells ($p = 0.046$; Figure 3C). We also noted that the IL13BBζ T cells caused no overt toxicities when intracranially administered in these mouse models, a point of interest in light of the potential of human IL13(E13Y)-containing CARs to cross-react with murine IL13Rα1 and IL13Rα2 (Figure S3 and Krebs et al.[20]), and the reported expression of IL13Rα1 in both murine and human brain.[32,33] This lack of toxicity is also consistent with the favorable safety profile thus far observed in patients treated with IL13Rα2-targeted CAR T cells.[21,22]

In an effort to estimate the ratio of T cells to tumor cells that produced an effective anti-tumor response in these experiments, we extracted two PBT030-2 tumors at day 8 of engraftment. The average tumor volume in this experiment was 1.67×10^7 μm^3. Based on reconstruction of multiple H&E-stained sections and calculations made with software as described in the Materials and Methods, we estimated that a 1.67×10^7 μm^3 tumor volume corresponded to approximately 0.17×10^6 tumor cells. Thus, since 0.1×10^6 CAR^+ IL13BBζ T cells eradicated a tumor consisting of almost 0.2×10^6 cells, we calculated that a ratio of approximately 1 CAR^+ T cell to 2 tumor cells was sufficient for eradicating orthotopic GBM in this model.

Immunohistochemical analysis of brains harvested from mice 6 days after ICT treatment also revealed significantly increased numbers of $CD3^+$ T cells detected throughout the brain (20-fold increase) and at the tumor site (13-fold increase) of mice treated with IL13BBζ T cells, as compared to those treated with the IL13ζ $CD8^+$ clone 2D7 (Figures 3E and 3F). Besides residing within the tumor, these $CD3^+$ IL13BBζ T cells were commonly found in the corpus callosum and leptomeninges, including the choroid plexus and ependymal lining (Figure 3E). This improved persistence for second-generation IL13BBζ T cells is also supported by in vitro co-culture assays, which detected significantly greater numbers of viable IL13BBζ T cells, as compared to IL13ζ $CD8^+$ CTL, following IL13Rα2^+ tumor cell killing (Figure S4).

CAR Enrichment Is Not Necessary for Therapeutic Efficacy

We next investigated whether pre-enrichment of CAR-expressing T cells prior to adoptive transfer was necessary for optimal anti-tumor activity when administering a specified CAR^+ T cell dose. NSG mice receiving 2×10^5 CAR^+ cells from an IL13BBζ T cell population that was either 10% CAR^+ or enriched to be 100% CAR^+ exhibited similar anti-tumor responses, with only one out of six mice from the 10% CAR^+ group not responding to treatment (Figure 4). Indeed, there was not a statistical difference between the 10% CAR^+ and 100% CAR^+ groups when comparing either tumor flux at day 41 ($p = 0.3849$; Figure 4B) or overall survival ($p = 0.3613$; Figure 4C). Thus, these data suggest that, when dosing is based on CAR positivity, CAR enrichment is not necessary for therapeutic efficacy.

Evaluating Impact of Dexamethasone on Therapeutic Potency of IL13BBζ T Cells

Because IL13Rα2-targeted GBM immunotherapy is currently being evaluated in early-stage clinical trials, where many patients receive dexamethasone to decrease edema and counter symptoms and/or adverse events, we evaluated the effects of corticosteroids on CAR T cell treatment in our PBT030-2 tumor xenograft model. Five days after introduction of $ffLuc^+$ PBT030-2 cells, daily injections of high, mid, or low levels of dexamethasone (5, 1, or 0.2 mg/kg, respectively) were initiated and continued for 4 weeks, with one dose of IL13BBζ T cells administered on day 8 (Figure 5). Complete loss of CAR T cell-mediated effects was only observed in mice that received the highest dose of dexamethasone (5 mg/kg). Mice given the more clinically relevant dexamethasone doses of 1 or 0.2 mg/kg continued to exhibit tumor growth control by bioluminescent imaging up to day 63 (Figures 5A and 5B) and showed a significant survival benefit (Figure 5C). While the survival of mice treated with mid or low levels of dexamethasone may have been modestly reduced compared to mice not treated with dexamethasone, this difference was not statistically significant (Figure 5C). Thus, overall, these data suggest that in vivo anti-tumor effects of CAR T cells against brain tumors can be maintained in the presence of low-dose dexamethasone.

Evaluating Impact of Delivery Route on Therapeutic Potency of IL13BBζ T Cells

Because T cells have been shown to have the capacity to traffic to tumors[34,35] and intravenous (IV) infusions would be significantly less invasive than intracranial infusions when translating CAR T cell therapy to the clinic for GBM, we compared these two routes of IL13BBζ T cell delivery in our orthotopic PBT030-2 tumor xenograft model (Figure 6). In contrast to that observed with ICT administration, there was no therapeutic efficacy observed with IV administered CAR T cells (Figures 6A and 6B). Experiments performed with smaller tumors (i.e., engrafted for 8 days instead of the 19 days depicted in Figure 6) exhibited the same result (data not shown). Immunohistochemical analysis suggests that IV administered IL13BBζ T cells do not traffic to the tumor site as efficiently as do ICT administered cells (Figure 6C). Thus, local delivery of IL13BBζ T cells appears to be superior to systemic delivery for treatment of GBM.

We next compared two different routes of local intracranial delivery, either to the tumor site (ICT) or the ventricular system (intraventricularly [ICV]). For these studies, we used a multifocal GBM model, injecting $ffLuc^+$ PBT030-2 tumor cells into both the left and right hemispheres of the mouse brain, and evaluated the efficacy of a single infusion of IL13BBζ T cells either ICV or to the right ICT (Figure 7). Xenogen imaging of the left versus right hemispheres of the brain revealed that both ICT and ICV CAR T cells inhibited the growth of the tumor on the right, but ICV administration more efficiently affected the growth of the contralateral tumor on the left (Figure 7C).

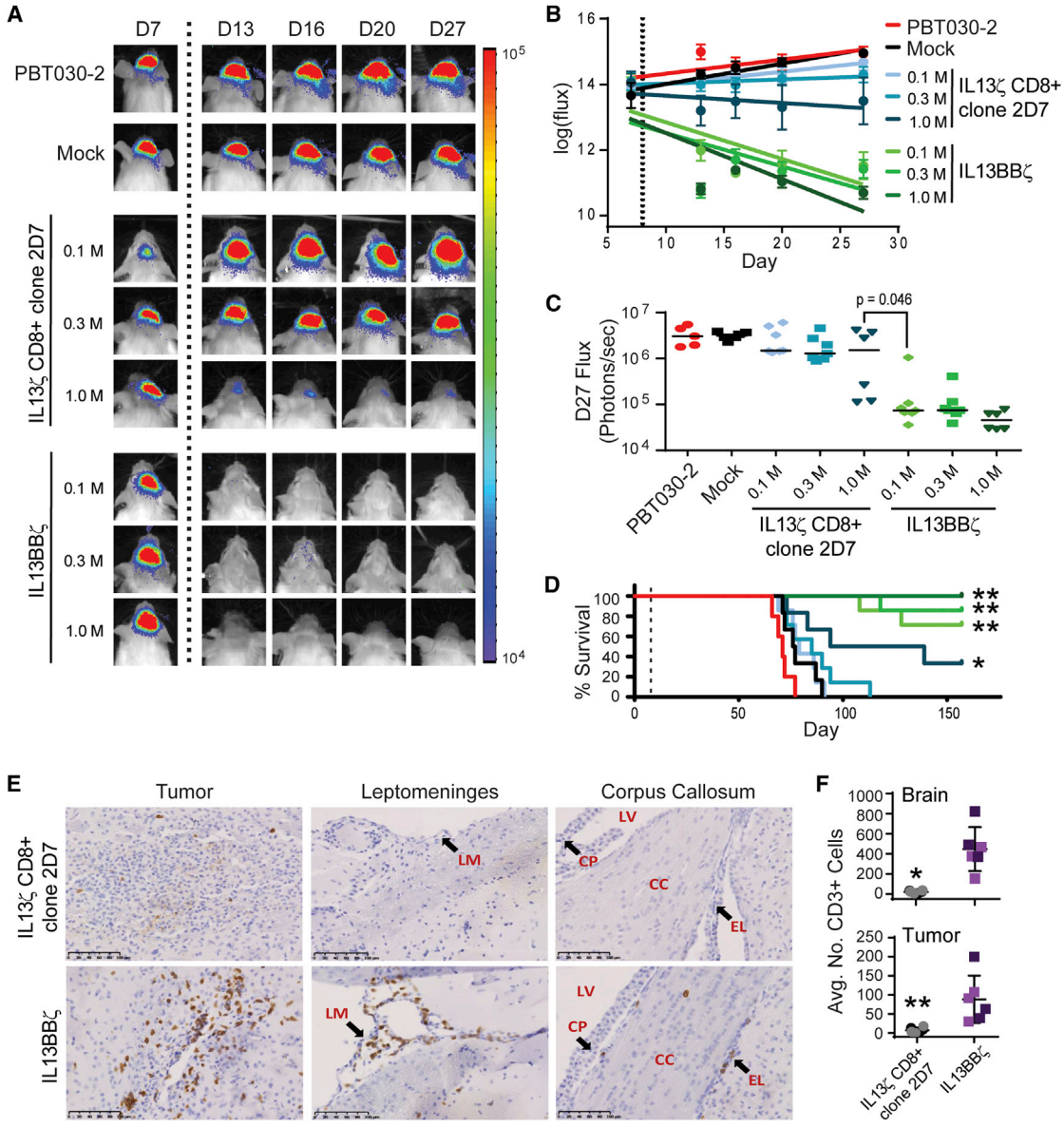

Figure 3. IL13BBζ T Cells Mediate Superior Anti-tumor Efficacy as Compared to First-Generation IL13ζ T Cells

ffLuc$^+$ PBT030-2 cells (1×10^5) were stereotactically implanted into the right forebrain of NSG mice. On day 8 (A–D) or day 5 (E and F), mice (n = 6 or 7 per group) received either no treatment (PBT030-2); ICT treatment with 1.6×10^6 mock-transduced T cells (Mock); 0.1×10^6, 0.3×10^6, or 1.0×10^6 IL13ζ CD8$^+$ clone 2D7 cells; or 0.1×10^6, 0.3×10^6, or 1.0×10^6 CAR$^+$ IL13BBζ T cells (1.0×10^6 CAR$^+$ = 1.6×10^6 total T cells; 63% CAR$^+$). (A) Representative mice from each group showing relative tumor burden over time using Xenogen Living Image. T cell infusion on day 8 is indicated by the vertical dotted line. (B) Linear regression lines of the natural log of ffLuc flux (photons/s) for each group over time. T cell infusion on day 8 is indicated by the dotted vertical line, and means ± SE are depicted at each time point. (C) Quantification of ffLuc flux on day 27. Each data point represents an individual mouse, and lines indicate median values. p = 0.046 when comparing mice treated with 1.0×10^6 IL13ζ CD8$^+$ clone 2D7 to those treated with 0.1×10^6 CAR$^+$ IL13BBζ T cells using an unpaired Student's t test. (D) Kaplan-Meier survival analysis demonstrating improved survival for mice treated with IL13BBζ T cells. T cell infusion on day 8 is indicated by the dotted vertical line. *p = 0.048; **p ≤ 0.005 when compared to mice treated with mock-transduced T cells using the log rank (Mantel-Cox) test. (E) Representative 20× immunohistochemical images of brains collected from mice 6 days after ICT treatment with 1.0×10^6 IL13ζ CD8$^+$ clone 2D7 cells or CAR$^+$ IL13BBζ T cells (1.0×10^6 CAR$^+$ = 3.0×10^6 total T cells; 33% CAR$^+$) and stained for CD3$^+$ T cells. Sites of tumor (left), leptomeninges (LM, center), and corpus callosum (CC, right) each with 100 μm scale bars are depicted. LV, lateral ventricle; CP, choroid plexus; EL, ependymal lining. (F) Average CD3 cell counts (±SD) from either the whole-brain section (top) or tumor-containing field (bottom) were determined from the experiment described in (E) using two brains per group and three sections per brain. *p = 0.0008; **p = 0.0099 when compared to mice treated with IL13BBζ T cells using an unpaired Student's t test.

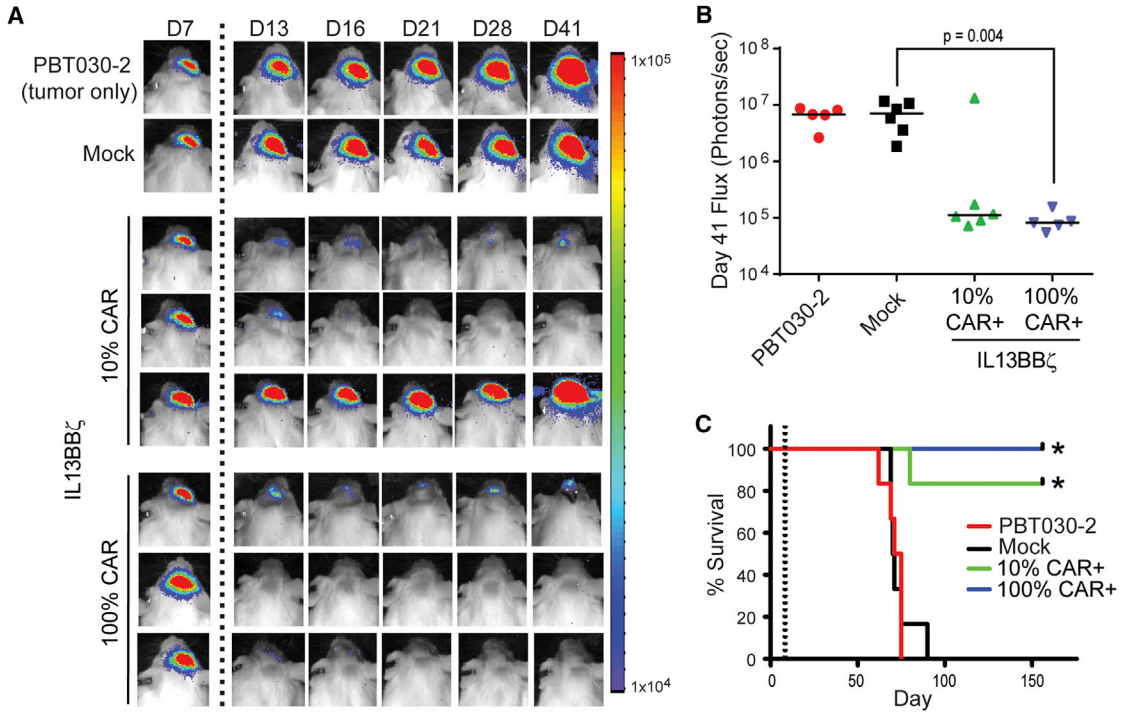

Figure 4. Proportion of Cells That Are CAR$^+$ Does Not Impact Therapeutic Efficacy

ffLuc$^+$ PBT030-2 cells (1×10^5) were stereotactically implanted into the right forebrain of NSG mice. On day 8, mice (n = 5 or 6 per group) received no treatment (PBT030-2) or ICT treatment with either 2×10^6 mock-transduced T cells (Mock) or 0.2×10^6 CAR$^+$ IL13BBζ T cells—either 2×10^6 total cells of a 10% CAR$^+$ population or 0.2×10^6 total cells of a 100% CAR$^+$ population. (A) Representative mice from each group showing relative tumor burden over time using Xenogen Living Image. T cell infusion on day 8 is indicated by the vertical dotted line. (B) Quantification of ffLuc flux on day 41. Each data point represents an individual mouse, and lines indicate median values. Using an unpaired Student's t test, p = 0.385 when comparing the 10% and 100% CAR$^+$ groups, and p = 0.004 when comparing the Mock and 100% CAR$^+$ groups. (C) Kaplan-Meier survival curve demonstrating significantly improved survival for mice treated with either the 10% or 100% CAR$^+$ IL13BBζ T cells. T cell infusion on day 8 is indicated by the vertical dotted line. *p ≤ 0.0015 when compared to mock-transduced T cells using the log rank (Mantel-Cox) test. No significant difference in survival between the 10% CAR$^+$ and 100% CAR$^+$ groups was observed (p = 0.3613).

Tumor sizes based on H&E staining of brains harvested 7 days after T cell infusion also showed similar IL13BBζ T cell-mediated tumor control on the right with both ICT and ICV administration, and on the left with only ICV administration (Figure 7D). This result was not tumor specific, as similar results were seen with a multifocal ffLuc$^+$ U251T model (Figure S5). Interestingly, however, CD3$^+$ T cells were detected in both the right and left tumor sites in both groups of mice when examined 7 days after IL13BBζ T cell infusion (Figure 7E). Furthermore, the survival rates of the ICT- versus ICV-treated groups were not statistically different from each other (p = 0.4187) (Figure 7F).

DISCUSSION

The goal of this study was to pre-clinically evaluate parameters of CAR T cell therapy related to its clinical translation to the treatment of brain tumors. These findings have informed clinical trial design and provided the rationale for our recently initiated clinical trial utilizing next-generation IL13BBζ T cells to treat GBM (NCT02208362). Early clinical observations are encouraging, with demonstrated safety and evidence for anti-tumor activity, including one patient who exhibited a complete response against recurrent multifocal GBM.[22]

For these studies, we generated a fully human second-generation IL13(E13Y)-ligand-based CAR that incorporated a 4-1BB (CD137) co-stimulatory domain[36] to enhance anti-tumor potency and mutations in the IgG4 Fc spacer (L235E, N297Q) to reduce binding to Fc gamma receptors (FcγRs).[24] We also chose an enriched Tcm population for lentiviral genetic engineering on the basis of studies using both murine xenograft models and a non-human primate model relevant for human translation, where adoptively transferred effector T cells derived from sort-purified CD62L$^+$ Tcm were found to persist in the blood and responded to antigen challenge in vivo.[27,29] Here, we observe that autologous Tcm-derived IL13BBζ T cells retained their memory phenotype after their genetic modification and ex vivo propagation. Further, we provide evidence that IL13BBζ T cells mediate IL13Rα2-redirected effector function with minimal targeting of IL13Rα1. IL13BBζ T cells were preferentially activated by plate-bound IL13Rα2-Fc, as compared to IL13Rα1-Fc, when challenged at equivalent receptor concentrations and did not produce

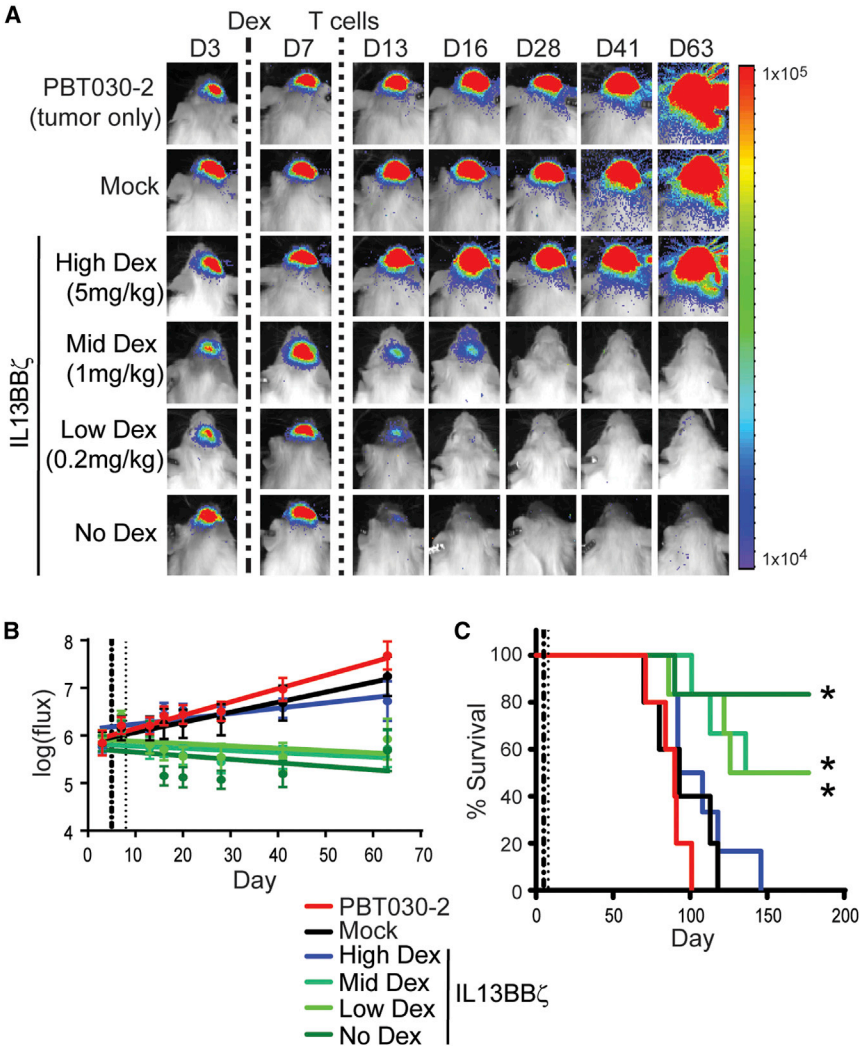

Figure 5. Impact of Dexamethasone on CAR T Cell In Vivo Anti-tumor Activity

ffLuc$^+$ PBT030-2 cells (1×10^5) were stereotactically implanted into the right forebrain of NSG mice. On day 5, mice that were to receive CAR$^+$ T cells initiated daily s.c. injections of dexamethasone (Dex) at different doses—High Dex (5 mg/kg, n = 6), Mid Dex (1 mg/kg, n = 6), Low Dex (0.2mg/kg, n = 6), or No Dex (n = 6)—for a total of 4 weeks. On day 8, mice received no treatment (PBT030-2, n = 5) or ICT treatment with either 0.37×10^6 mock-transduced T cells (Mock, n = 5) or 0.3×10^6 CAR$^+$ IL13BBζ T cells (0.37×10^6 total cells, 78% CAR$^+$; n = 24). (A) Representative mice from each group showing relative tumor burden over time using Xenogen Living Image. Initiation of Dex infusions on day 5 is indicated by the vertical dash-dot line; T cell infusion on day 8 is indicated by the vertical dotted line. (B) Linear regression lines of the natural log of ffLuc flux (photons/s) for each group over time. Initiation of Dex infusions on day 5 is indicated by the vertical dash-dot line, T cell infusion on day 8 is indicated by the vertical dotted line, and means ± SD are depicted at each time point. (C) Kaplan-Meier survival curve demonstrating improved survival for No, Low, and Mid Dex-treated mice. Initiation of Dex infusions on day 5 is indicated by the vertical dash-dot line; T cell infusion on day 8 is indicated by the vertical dotted line. *$p \leq 0.02$ when compared to mock-transduced T cells using the log rank (Mantel-Cox) test. No significant difference in survival between the High Dex and Mock groups (p = 0.52) nor between the Mid or Low Dex and No Dex groups (p = 0.39 or 0.30, respectively) was observed.

inflammatory cytokines or efficiently kill when co-cultured with cells that endogenously express IL13Rα1. This finding is important for the anticipated clinical safety of this ligand-based CAR platform and is in contrast to pre-clinical data from other groups in which similar IL-13-mutein ligand-CARs cross-reacted with IL13Rα1,[20,37] suggesting that differences in CAR design outside the tumor targeting domain may contribute to selective recognition. Ongoing studies are focused on evaluating the impact of CAR expression levels and CAR design features, including linker length and co-stimulatory domain, on IL13Rα2-selective recognition.

One of our primary objectives of this study was to improve anti-tumor activity and persistence as compared to our first-generation IL13ζ CD8$^+$ T cells, a CAR T cell product that has been evaluated in nine patients under two phase I clinical trials (NCT00730613, NCT01082926). The clinical testing of IL13ζ CD8$^+$ T cells for the treatment of GBM represented the first application of CAR T cells for the treatment of brain tumors. Those initial studies were highly informative, as they demonstrated the safety of repetitive intracranial delivery of IL13ζ CD8$^+$ T cells,[21] and they were the first to track CAR T cells following intracranial adoptive transfer by engineering cells to co-express the herpes simplex virus 1 thymidine kinase reporter gene (HSV1-TK) which allowed positron emission tomography (PET) imaging with 9-[4-[18F]fluoro-3-(hydroxymethyl)butyl]guanine ([18F]FHBG).[38,39] Evidence for anti-glioma bioactivity was also found, as suggested by significant loss of IL13Rα2$^+$ tumor cells in one patient and increased tumor necrotic volume in a second patient.[21] However, although these findings are encouraging, the first-generation product showed limited persistence following adoptive transfer in pre-clinical models, and we hypothesized that low T cell persistence may have limited clinical outcomes. In this study, we have now demonstrated that our next-generation IL13BBζ T cells significantly outperform first-generation IL13ζ CD8$^+$ T cells against orthotopic patient-derived GBM, with improved persistence post-adoptive transfer.

Clinical dosing of CAR T cells is commonly based on CAR positivity. However, the impact of un-engineered, or CAR-negative T cells on anti-tumor potency, particularly when the cells are delivered directly to the tumor site, has not been established. To test this impact, we

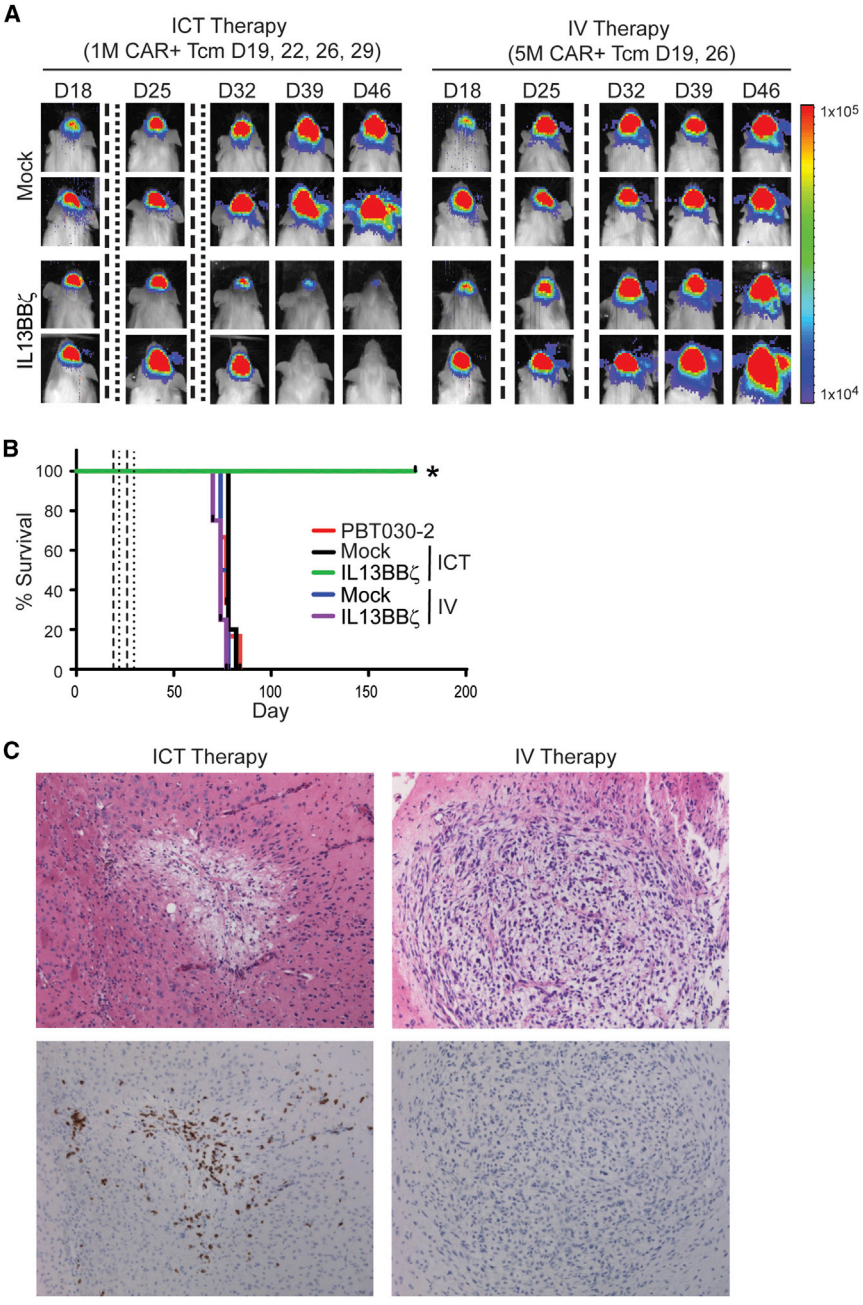

Figure 6. Therapeutic Efficacy Observed with ICT, but Not IV, CAR T Cell Administration

ffLuc$^+$ PBT030-2 cells (1×10^5) were stereotactically implanted into the right forebrain of NSG mice. Treated mice received either mock-transduced or IL13BBζ T cells either ICT on days 19, 22, 26, and 29 (1×10^6 CAR$^+$ cells) or IV on days 19 and 26 (5×10^6 CAR$^+$ cells). (A) Representative mice from each T cell-treated group (n = 6/group) showing relative tumor burden over time using Xenogen Living Image. T cell infusions on days 19 and 26 are indicated by the vertical dashed lines; T cell infusions on days 22 and 29 are indicated by the vertical dotted lines. (B) Kaplan-Meier survival curve demonstrating improved survival for ICT IL13BBζ T cell-treated mice. T cell infusions on days 19 and 26 are indicated by the vertical dashed lines; T cell infusions on days 22 and 29 are indicated by the vertical dotted lines. *p = 0.0035 when compared to ICT delivered mock-transduced T cells using the log rank (Mantel-Cox) test. (C) Representative 10× images of H&E (top)- and CD3 IHC (bottom)-stained tumor sites of brains harvested 7 days after the last ICT (left) or IV (right) IL13BBζ T cell administration.

compared the anti-tumor activity of a set CAR$^+$ T cell dose that was formulated from either a 100% CAR$^+$ population or a 10% CAR$^+$ population. Our findings suggest that, even in the setting of intracranial injections to the tumor site, the presence of a large proportion of CAR-negative T cells in a cell product formulation (i.e., as in that derived from a 10% CAR$^+$ population) does not affect the anti-tumor potency or survival benefit of adoptive therapy with IL13BBζ T cells. Thus, dosing by CAR positivity appears to obviate the need to enrich for a 100% CAR-expressing T cell product, and we intend to continue with this dosing strategy in clinical trials going forward.

To further inform our clinical trial design, we also examined the extent to which dexamethasone may affect the function of our CAR T cells, as many GBM patients are treated with this steroid to decrease edema and improve symptoms,[40] and yet it is also known to regulate T cell growth and differentiation.[41] Interestingly, anti-tumor responses and survival of IL13BBζ T cell-treated mice given 0.2 mg/kg or 1 mg/kg of dexamethasone were not significantly impaired as compared to the no-dexamethasone control group. These doses would correspond to 15 mg and 75 mg dexamethasone per day, respectively, for a patient weighing 75 kg. Therefore, since a dose of 10–20 mg dexamethasone is typically administered to brain tumor patients at the onset of acute neurological symptoms, followed by 4–24 mg of daily maintenance therapy,[42] our data suggest that CAR T cell anti-tumor function would not be substantially impaired with this standard-of-care dosing strategy. Although further understanding of the clinical impact of dexamethasone on CAR T cell therapy remains under investigation, based on the pre-clinical studies presented here, our clinical protocol (NCT02208362) allows for patients to be on a stable low dose of dexamethasone of $\leq$6 mg/day.

The optimal delivery route of CAR T cells for the treatment of brain tumors remains an outstanding question. The brain is an immune-specialized organ, with the blood-brain barrier functioning to regulate interactions between the immune system and the CNS (reviewed in Banks and Erickson[43]). Most ongoing CAR clinical trials for the

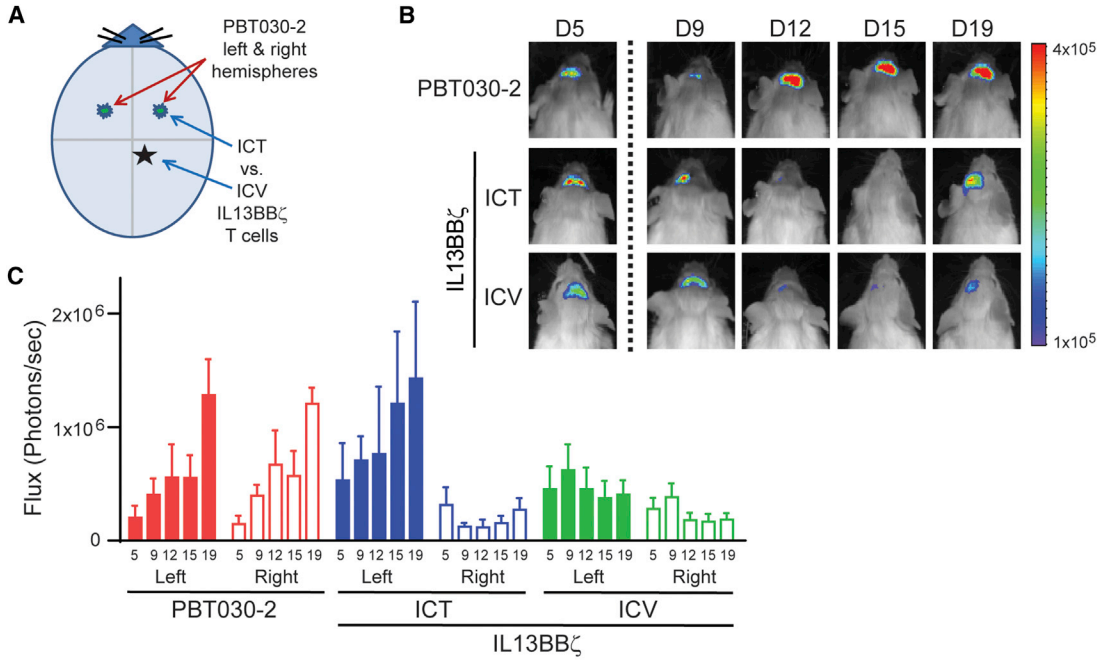

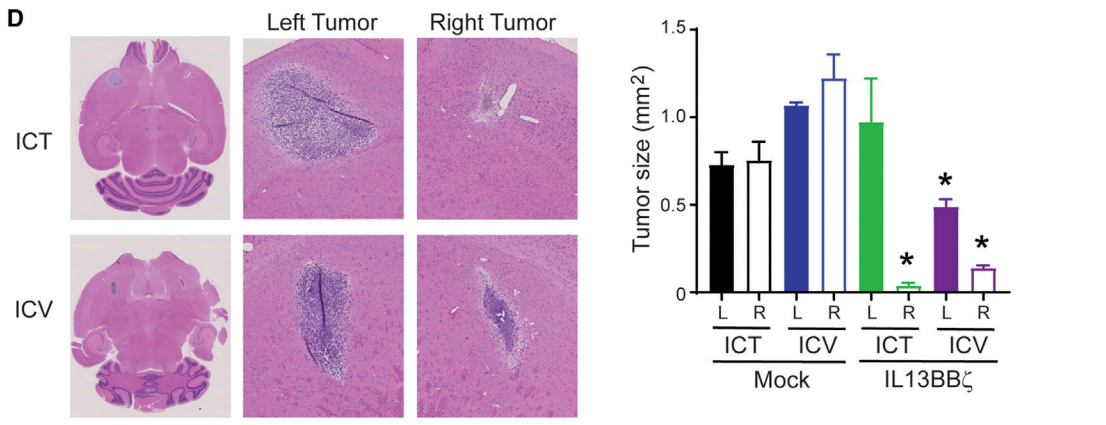

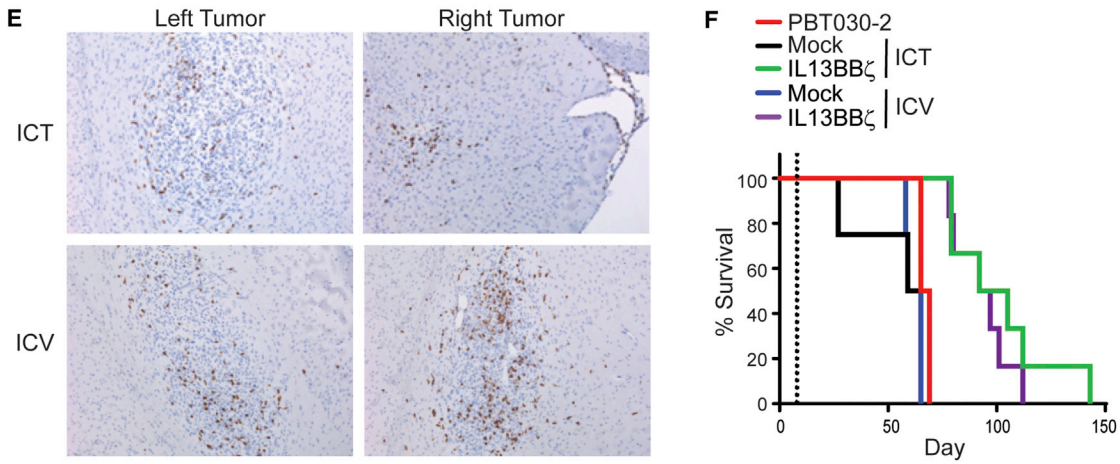

(legend on next page)

treatment of GBM (NCT01109095, NCT01454596, NCT02844062, NCT02209376)[44,45] are delivering CAR T cells IV. Systemic IV delivery is supported by CD19-CAR T cells trafficking to the CSF and reducing CNS leukemic disease burden,[6,8,46] as well as TILs eliminating melanoma tumors that had metastasized to the brain.[10] However, in both of these scenarios, the adoptively transferred T cells were likely primed by systemic tumors. For primary brain tumors, this would likely not be the case, and since resting T cells are known to not efficiently traffic to the CNS,[47] the efficiency of CAR T cell trafficking to the CNS might be highly dependent on their activation status after ex vivo manufacturing. Based on this, we directly tested the potency of IV versus intracranially administered CAR T cells and found that IV administration of our IL13BBζ T cells was ineffective, apparently due to inefficient cell trafficking to the intracranial tumors. In contrast, ICT administration of these CAR T cells provided long-term survival in mice. Although our findings may be influenced by our CAR design, manufacturing platform or the orthotopic models of GBM in immunocompromised mice, other groups have also demonstrated a benefit for locoregional delivery of CAR T cells for the treatment of solid tumors.[48,49] Therefore, these studies provide the rationale for continuing to evaluate local intracranial delivery in patients. Our earlier clinical trials with first-generation IL13Rα2-targeting CAR T cells utilized a Rickham catheter for ICT administration,[21,38] with no dose-limiting toxicities observed. Indeed, avoiding systemic IV delivery of CAR T cells may help decrease the risk of off-target side effects.

When considering a locoregional delivery approach for the treatment of GBM, we set out to compare intratumoral (ICT) delivery versus CSF delivery into the ventricles (ICV). We reasoned that CSF perfusion throughout the CNS might allow for better control of multifocal disease. Our findings in the multifocal orthotopic mouse model show that anti-tumor efficacy and improved survival can occur with either ICT or ICV delivery, yet ICV delivery appeared to better control the growth of the contralateral/distal tumor. Interestingly, our recently published case report suggests that while local delivery controlled local disease, ICV delivery mediated regression of multifocal lesions.[22] A more thorough clinical understanding of the effect of the route of delivery on CAR T cell safety and anti-tumor activity is highly warranted. As such, we are currently testing three different local delivery strategies in our ongoing clinical trial—ICT, ICV, and dual ICT/ICV (NCT02208362).

All together, the results of these studies have set the stage for our most recently initiated clinical trial utilizing second-generation IL13BBζ T cells to treat GBM (NCT02208362). Having developed several optimizations to our IL13Rα2-directed CAR T cell product, with the objective of improving therapeutic efficacy through augmenting persistence and activity, this work has provided the groundwork to now evaluate IL13BBζ T cells and their potential clinical benefit for a patient population that is greatly in need of novel therapeutics. Furthermore, while these findings are being directly applied to GBM patients at our institution, they also provide general insights into the translation of CAR T cell therapy for malignant brain tumors.

MATERIALS AND METHODS

CAR Construct

The codon-optimized IL-13(E13Y) mutein-containing IL13-zetakine CAR sequence was previously described[21] and is here referred to as *IL13ζ*. The ribosomal skip *T2A* sequence[26] was fused by PCR splice overlap extension to the truncated *CD19t* sequence obtained from the leader peptide to the transmembrane-spanning components (i.e., base pairs 1–972) of a *CD19*-containing plasmid. The *IL13ζ* and *T2A-CD19t* fragments were ligated into the previously described epHIV7 lentiviral vector.[30] The *4-1BB* co-stimulatory sequence was then inserted by splice overlap PCR, and then that construct underwent sequential site-directed mutagenesis using the QuikChange II XL kit (Agilent Technologies, Santa Clara, CA) to generate *IL13(E13Y)-IgG4(L235E,N297Q)-CD4tm-41BB-Zeta-T2A-CD19t_epHIV7*, which we refer to here as *IL13(EQ)BBZ-T2A-CD19t_epHIV7*.

CliniMACS Immunomagnetic Tcm Enrichment

Blood products were obtained from healthy donors under protocols approved by the City of Hope (COH) Internal Review Board. Peripheral blood mononuclear cells (PBMCs) were isolated by density gradient centrifugation over Ficoll-Paque (GE Healthcare, Little Chalfont, UK) and then underwent sequential rounds of CliniMACS/AutoMACS depletion (to remove $CD45RA^+$ naive T cells, $CD25^+$ regulatory T cells, and $CD14^+$ monocytes) and selection to enrich for the $CD45RO^+$ $CD62L^+$ Tcm population. In brief, PBMCs were incubated with clinical-grade anti-CD25, anti-CD14, and anti-CD45RA microbeads (Miltenyi Biotec, Bergisch Gladbach, Germany) for 30 min at room temperature (RT) in X Vivo15 media (BioWhittaker, Walkersville, MD) containing 10% fetal calf serum (FCS) (HyClone, GE Healthcare).

Figure 7. Therapeutic Efficacy Observed with ICT and ICV CAR T Cell Administration

$ffLuc^+$ PBT030-2 cells (1×10^5) were stereotactically implanted into both the left and right forebrains of NSG mice. Treated mice received either mock-transduced or IL13BBζ T cells (1×10^6 CAR^+ cells) either ICT or ICV on day 6 (B, C, and E) or day 8 (D and F). (A) Schematic of tumor cell and T cell intracranial injection sites. (B) Representative mice from each group (n = 5 per group) showing relative tumor burden over time using Xenogen Living Image. T cell infusion on day 6 is indicated by the vertical dotted line. (C) Quantification of mean ffLuc flux (+SE) on days 5, 9, 12, 15, and 19 (indicated on the x axis) for each brain hemisphere (left or right) in the untreated (red), ICT-treated (blue), and ICV-treated (green) groups of mice. (D) Representative 0.68× and 5× images of H&E staining of tumors in brains harvested 7 days after IL13BBζ T cell administration either ICT (top) or ICV (bottom). Images such as these were then used to determine length × width calculations of tumor area (mm^2) in both the left (L) and right (R) hemispheres of mice treated with either mock-transduced or IL13BBζ T cells as depicted in the graph (mean + SD). *$p < 0.0111$ when compared to the respective hemisphere and delivery of mock-transduced T cells using the unpaired Student's t test. (E) Representative 10× images of CD3 IHC stained tumor sites (left versus right) of brains harvested 7 days after IL13BBζ Tcm administration either ICT (top) or ICV (bottom). (F) Kaplan-Meier survival curve demonstrating improved survival for IL13BBζ T cell-treated mice. T cell infusion on day 8 is indicated by the vertical dotted line. Using the log rank (Mantel-Cox) test, $p = 0.0018$ when comparing IL13BBζ to mock-transduced T cell treatment given either ICT or ICV; $p = 0.4187$ when comparing IL13BBζ T cell treatment given either ICT or ICV.

$CD25^+$, $CD14^+$, and $CD45RA^+$ cells were then immediately depleted using the CliniMACS depletion mode according to the manufacturer's instructions (Miltenyi Biotec). After centrifugation, the unlabeled negative fraction of cells was resuspended in CliniMACS PBS/EDTA buffer (Miltenyi Biotec) containing 0.5% human serum albumin (HSA) (CSL Behring, King of Prussia, PA) and then labeled with clinical grade biotinylated-DREG56 monoclonal antibody (mAb) (City of Hope Center for Biomedicine and Genetics) at 0.1 μg/10^6 cells for 30 min at RT. The cells were then washed and resuspended in a final volume of 100 mL CliniMACS PBS/EDTA containing 0.5% HSA. After 30 min incubation with 1.25 mL anti-biotin microbeads (Miltenyi Biotec), the $CD62L^+$ fraction (Tcm) was purified with positive selection on CliniMACS according to the manufacturer's instructions and resuspended in X Vivo15 media containing 10% FCS.

Activation, Lentiviral Transduction, and Expansion of Enriched Tcm

Tcm were stimulated with Dynabeads Human T expander CD3/CD28 (Invitrogen, Carlsbad, CA) at a 1:3 ratio (T cell:bead) and transduced with IL13(EQ)BBZ-T2A-CD19t_epHIV7 at an MOI of 0.3 or greater in X Vivo15 containing 10% FCS with 5 μg/mL protamine sulfate (APP Pharmaceuticals, Schaumburg, IL), 50 U/mL rhIL-2, and 0.5 ng/mL rhIL-15. Cultures were then maintained at 37°C, 5% CO_2, with addition of X-Vivo15, 10% FCS as required to keep cell density between 3×10^5 and 2×10^6 viable cells/mL, with cytokine supplementation (final concentration of 50 U/mL rhIL-2 and 0.5 ng/mL rhIL-15) every Monday, Wednesday, and Friday of culture. On day 7+ of culture, the CD3/CD28 Dynabeads were removed from cultures using the DynaMag-50 magnet (Invitrogen). Cultures were propagated for up to 28 days prior to cryopreservation.

Cell Lines

Generation of Epstein-Barr virus (EBV)-transformed LCLs and LCLs that express a membrane-tethered CD3 epsilon-specific scFv agonist OKT3 (LCL-OKT3) have been previously described.[29,50] The low-passage GBM tumor sphere line PBT030-2 and PBT030-2 engineered to express the ffLuc reporter gene have been previously described.[19] The low-passage GBM tumor sphere line PBT103-2-Rα2 was similarly derived from a patient sample but engineered to constitutively express both human IL13Rα2 and ffLuc. Fibrosarcoma line HT-1080 and chronic myelogenous leukemia line K-562 were obtained from the American Tissue Culture Collection (ATCC) and maintained according to their recommendations, with HT-1080 and K-562 cells lentivirally transduced to express IL13Rα2 by using an IL13Ra2-T2A-eGFP-ffLuc_pHIV7 construct and standard methods. U251T GBM cells were previously described.[11]

Generation of the $IL13\zeta^+$ $CD8^+$ clone 2D7 was previously described.[18] Briefly, this line was derived from human PBMCs that had undergone OKT3 activation, electroporation with an IL13-zetakine/HyTK-pMG plasmid, and subsequent cloning and propagation in hygromycin/rhIL-2.[18,51]

Flow Cytometric Analysis

Effector cells were stained with fluorochrome-conjugated monoclonal antibodies (mAbs) to either human CD3, CD4, CD8, CD28, IL-13, TCRα/β (BD Biosciences, San Jose, CA), CD19 (Beckman Coulter, Brea, CA), or CD62L (ThermoFisher Scientific, Carlsbad, CA). Tumor cells were stained with goat anti-human IL13Rα1 or IL13Rα2 (R&D Systems, Minneapolis, MN), followed by phycoerythrin-conjugated donkey anti-goat antibody (Novus Biologicals, Littleton, CO). Isotype-matched mAbs served as controls. Data acquisition was performed on a FACS Calibur instrument (BD Biosciences) using FCS Express V3 Software (De Novo Software, Los Angeles, CA).

Cytotoxicity Assays

^{51}Cr release assays were performed as previously described[52] using the indicated effector cells and ^{51}Cr-labeled target cells.

Cytokine Production Assays

Freshly thawed T cell products (10^6) were co-cultured overnight in 48-well tissue culture plates with 10^5 of the indicated stimulator cells. In some experiments, tumor cells alone were cultured for 72 hr. Harvested supernatants were analyzed by cytometric bead array using the Human Cytokine 10-Plex Panel (Invitrogen) according to the manufacturer's instructions.

In some experiments, T cells were cultured overnight at 5×10^3 cells per well on 96-well plates that had been coated with 5,000, 2,500, 1,250, 625, or 312.5 ng/mL recombinant human IL13Rα1-Fc chimera or IL13Rα2-Fc chimera (R&D Systems). Supernatants were then evaluated for IFN-γ levels using the Legend Max ELISA kit with pre-coated plates (Human IFN-γ) (Biolegend, San Diego, CA).

Xenograft Models

All mouse experiments were approved by the COH Institute Animal Care and Use Committee. On day 0, $ffLuc^+$ PBT030-2 cells (1×10^5) were stereotactically implanted into the right forebrain of NSG mice. The multifocal model involved injection of 1×10^5 $ffLuc^+$ PBT030-2 cells to both the right and left forebrains of each mouse. Mice were then treated intratumorally (i.e., intracranially, ICT), IV, or ICV with $0.2–2.0 \times 10^6$ CAR T cells as indicated for each experiment. In some experiments, some groups of mice also received 4 weeks of daily subcutaneous (s.c.) injections of dexamethasone (at 0.2, 1, or 5 mg/kg) starting at day 5. Groups of mice were then monitored for tumor engraftment by Xenogen non-invasive optical imaging as previously described[18] or for survival, with euthanasia applied according to the American Veterinary Medical Association Guidelines.

Calculating Tumor Cell Number Based on Volume

Harvested PBT030-2 brain tumors were paraffin embedded and approximately 30 sections (10 μm thick, 100 μm apart) were made of each tumor and stained with H&E. Sections were scanned at 40× magnification (average image size 200 Mb) using a digital slide scanner NanoZoomer 2.0-HT: C9600 (Hamamatsu, Bridgewater, NJ), and sections containing tumor tissue were imported into software Voloom version 1.8.

Calculation of the cell numbers within each tumor was then based on the following: since the height of each section is 10 μm, the volume of each section equals area × 10 μm. NDP.view2 software (Hamamatsu) was used to acquire tumor section area (A) and then to manually count the cell number (C) within that area. We estimated that there were two layers of cells within each section, so the average single-cell volume would equal (section volume)/(2 × the cell count within tumor area), or (10 × A)/(2 × C). Using this equation, the average cell volume was determined to be 951.01 μm^3, which we rounded to 1,000 μm^3 for all future calculations. Since dense tumor tissue has strong blue staining because of its high nucleus/plasma ratio, Voloom version 1.8 can recognize that blue stain on the provided sections, construct a 3D model, and calculate total tumor volumes. The cell number within a PBT030-2 tumor was then estimated to equal (tumor volume)/1,000.

Immunohistochemistry

Harvested brains were paraformaldehyde fixed and embedded in paraffin. Horizontal brain sections (10 μm) were deparaffinized, quenched in 3% hydrogen peroxide, and pre-treated to promote antigen retrieval by steaming method (20 min in high pH, 50×). Slides were then incubated in Protein Block (Dako, Carpenteria, CA) and stained for 30 min with a monoclonal mouse anti-human CD3 antibody (1/200 in dilution buffer, Dako). After washing, the slides were incubated in Mouse Polymer (Dako), washed again, incubated with the chromogen diaminobenzidine tetrahydrochloride and then counterstained with hematoxylin prior to rehydration and mounting.

SUPPLEMENTAL INFORMATION

Supplemental Information includes five figures and one table and can be found with this article online at https://doi.org/10.1016/j.ymthe.2017.10.002.

AUTHOR CONTRIBUTIONS

Conceptualization, C.E.B., B.B., M.E.B., S.J.F.; Methodology, X.Y., B.A., L.W., W.-C.C.; Formal Analysis, X.Y., J.R.O., R.S., B.A.; Investigation, X.Y., B.A., R.S., W.-C.C., L.W., B.C., A.S., A.B.; Resources, M.D., B.B., M.E.B., S.J.F.; Writing – Original Draft, J.F.S.; Writing – Review and Editing, J.R.O.; Visualization, C.E.B., J.R.O.; Supervision, C.E.B., S.J.F.; Funding Acquisition, C.E.B., S.J.F.

CONFLICTS OF INTEREST

Patents associated with this work have been licensed by Mustang Bio., Inc., for which S.J.F. and C.E.B. receive royalty payments.

ACKNOWLEDGMENTS

We thank the Analytical Pharmacology, Animal Resource Center, Pathology, and Small Animal Imaging cores, as well as Suzette Blanchard and Yubo Zhai for their technical assistance. This work was supported by grants from the California Institute for Regenerative Medicine (CIRM; TR3-05641) and the NIH (P30 CA33572, cores).

REFERENCES

1. Dolecek, T.A., Propp, J.M., Stroup, N.E., and Kruchko, C. (2012). CBTRUS statistical report: primary brain and central nervous system tumors diagnosed in the United States in 2005-2009. Neuro-oncol. *14* (*Suppl 5*), v1–v49.
2. Batlevi, C.L., Matsuki, E., Brentjens, R.J., and Younes, A. (2016). Novel immunotherapies in lymphoid malignancies. Nat. Rev. Clin. Oncol. *13*, 25–40.
3. Maus, M.V., Grupp, S.A., Porter, D.L., and June, C.H. (2014). Antibody-modified T cells: CARs take the front seat for hematologic malignancies. Blood *123*, 2625–2635.
4. Ramos, C.A., Savoldo, B., and Dotti, G. (2014). CD19-CAR trials. Cancer J. *20*, 112–118.
5. Sadelain, M., Brentjens, R., Rivière, I., and Park, J. (2015). CD19 CAR therapy for acute lymphoblastic leukemia. Am. Soc. Clin. Oncol. Educ. Book *35*, e360–e363.
6. Lee, D.W., Kochenderfer, J.N., Stetler-Stevenson, M., Cui, Y.K., Delbrook, C., Feldman, S.A., Fry, T.J., Orentas, R., Sabatino, M., Shah, N.N., et al. (2015). T cells expressing CD19 chimeric antigen receptors for acute lymphoblastic leukaemia in children and young adults: a phase 1 dose-escalation trial. Lancet *385*, 517–528.
7. Maude, S.L., Frey, N., Shaw, P.A., Aplenc, R., Barrett, D.M., Bunin, N.J., Chew, A., Gonzalez, V.E., Zheng, Z., Lacey, S.F., et al. (2014). Chimeric antigen receptor T cells for sustained remissions in leukemia. N. Engl. J. Med. *371*, 1507–1517.
8. Grupp, S.A., Kalos, M., Barrett, D., Aplenc, R., Porter, D.L., Rheingold, S.R., Teachey, D.T., Chew, A., Hauck, B., Wright, J.F., et al. (2013). Chimeric antigen receptor-modified T cells for acute lymphoid leukemia. N. Engl. J. Med. *368*, 1509–1518.
9. Abramson, J.S., McGree, B., Noyes, S., Plummer, S., Wong, C., Chen, Y.B., Palmer, E., Albertson, T., Ferry, J.A., and Arrillaga-Romany, I.C. (2017). Anti-CD19 CAR T cells in CNS diffuse large-B-cell lymphoma. N. Engl. J. Med. *377*, 783–784.
10. Hong, J.J., Rosenberg, S.A., Dudley, M.E., Yang, J.C., White, D.E., Butman, J.A., and Sherry, R.M. (2010). Successful treatment of melanoma brain metastases with adoptive cell therapy. Clin. Cancer Res. *16*, 4892–4898.
11. Brown, C.E., Warden, C.D., Starr, R., Deng, X., Badie, B., Yuan, Y.C., Forman, S.J., and Barish, M.E. (2013). Glioma IL13Rα2 is associated with mesenchymal signature gene expression and poor patient prognosis. PLoS ONE *8*, e77769.
12. Debinski, W., Gibo, D.M., Hulet, S.W., Connor, J.R., and Gillespie, G.Y. (1999). Receptor for interleukin 13 is a marker and therapeutic target for human high-grade gliomas. Clin. Cancer Res. *5*, 985–990.
13. Thaci, B., Brown, C.E., Binello, E., Werbaneth, K., Sampath, P., and Sengupta, S. (2014). Significance of interleukin-13 receptor alpha 2-targeted glioblastoma therapy. Neuro-oncol. *16*, 1304–1312.
14. Wykosky, J., Gibo, D.M., Stanton, C., and Debinski, W. (2008). Interleukin-13 receptor alpha 2, EphA2, and Fos-related antigen 1 as molecular denominators of high-grade astrocytomas and specific targets for combinatorial therapy. Clin. Cancer Res. *14*, 199–208.
15. Jarboe, J.S., Johnson, K.R., Choi, Y., Lonser, R.R., and Park, J.K. (2007). Expression of interleukin-13 receptor alpha2 in glioblastoma multiforme: implications for targeted therapies. Cancer Res. *67*, 7983–7986.
16. Hegde, M., Mukherjee, M., Grada, Z., Pignata, A., Landi, D., Navai, S.A., Wakefield, A., Fousek, K., Bielamowicz, K., Chow, K.K., et al. (2016). Tandem CAR T cells targeting HER2 and IL13Rα2 mitigate tumor antigen escape. J. Clin. Invest. *126*, 3036–3052.
17. Krenciute, G., Krebs, S., Torres, D., Wu, M.F., Liu, H., Dotti, G., Li, X.N., Lesniak, M.S., Balyasnikova, I.V., and Gottschalk, S. (2016). Characterization and functional analysis of scFv-based chimeric antigen receptors to redirect T cells to IL13Rα2-positive glioma. Mol. Ther. *24*, 354–363.
18. Kahlon, K.S., Brown, C., Cooper, L.J., Raubitschek, A., Forman, S.J., and Jensen, M.C. (2004). Specific recognition and killing of glioblastoma multiforme by interleukin 13-zetakine redirected cytolytic T cells. Cancer Res. *64*, 9160–9166.
19. Brown, C.E., Starr, R., Aguilar, B., Shami, A.F., Martinez, C., D'Apuzzo, M., Barish, M.E., Forman, S.J., and Jensen, M.C. (2012). Stem-like tumor-initiating cells isolated from IL13Rα2 expressing gliomas are targeted and killed by IL13-zetakine-redirected T cells. Clin. Cancer Res. *18*, 2199–2209.
20. Krebs, S., Chow, K.K., Yi, Z., Rodriguez-Cruz, T., Hegde, M., Gerken, C., Ahmed, N., and Gottschalk, S. (2014). T cells redirected to interleukin-13Rα2 with interleukin-13

mutein—chimeric antigen receptors have anti-glioma activity but also recognize interleukin-13Rα1. Cytotherapy *16*, 1121–1131.

21. Brown, C.E., Badie, B., Barish, M.E., Weng, L., Ostberg, J.R., Chang, W.C., Naranjo, A., Starr, R., Wagner, J., Wright, C., et al. (2015). Bioactivity and safety of IL13Rα2-redirected chimeric antigen receptor $CD8^+$ T cells in patients with recurrent glioblastoma. Clin. Cancer Res. *21*, 4062–4072.
22. Brown, C.E., Alizadeh, D., Starr, R., Weng, L., Wagner, J.R., Naranjo, A., Ostberg, J.R., Blanchard, M.S., Kilpatrick, J., Simpson, J., et al. (2016). Regression of glioblastoma after chimeric antigen receptor T-cell therapy. N. Engl. J. Med. *375*, 2561–2569.
23. Debinski, W., and Thompson, J.P. (1999). Retargeting interleukin 13 for radioimmunodetection and radioimmunotherapy of human high-grade gliomas. Clin. Cancer Res. *5* (10, Suppl), 3143s–3147s.
24. Jonnalagadda, M., Mardiros, A., Urak, R., Wang, X., Hoffman, L.J., Bernanke, A., Chang, W.C., Bretzlaff, W., Starr, R., Priceman, S., et al. (2015). Chimeric antigen receptors with mutated IgG4 Fc spacer avoid fc receptor binding and improve T cell persistence and antitumor efficacy. Mol. Ther. *23*, 757–768.
25. van der Stegen, S.J., Hamieh, M., and Sadelain, M. (2015). The pharmacology of second-generation chimeric antigen receptors. Nat. Rev. Drug Discov. *14*, 499–509.
26. Donnelly, M.L., Luke, G., Mehrotra, A., Li, X., Hughes, L.E., Gani, D., and Ryan, M.D. (2001). Analysis of the aphthovirus 2A/2B polyprotein 'cleavage' mechanism indicates not a proteolytic reaction, but a novel translational effect: a putative ribosomal 'skip'. J. Gen. Virol. *82*, 1013–1025.
27. Berger, C., Jensen, M.C., Lansdorp, P.M., Gough, M., Elliott, C., and Riddell, S.R. (2008). Adoptive transfer of effector $CD8^+$ T cells derived from central memory cells establishes persistent T cell memory in primates. J. Clin. Invest. *118*, 294–305.
28. Graef, P., Buchholz, V.R., Stemberger, C., Flossdorf, M., Henkel, L., Schiemann, M., Drexler, I., Höfer, T., Riddell, S.R., and Busch, D.H. (2014). Serial transfer of single-cell-derived immunocompetence reveals stemness of CD8(+) central memory T cells. Immunity *41*, 116–126.
29. Wang, X., Berger, C., Wong, C.W., Forman, S.J., Riddell, S.R., and Jensen, M.C. (2011). Engraftment of human central memory-derived effector $CD8^+$ T cells in immunodeficient mice. Blood *117*, 1888–1898.
30. Wang, X., Naranjo, A., Brown, C.E., Bautista, C., Wong, C.W., Chang, W.C., Aguilar, B., Ostberg, J.R., Riddell, S.R., Forman, S.J., and Jensen, M.C. (2012). Phenotypic and functional attributes of lentivirus-modified CD19-specific human $CD8^+$ central memory T cells manufactured at clinical scale. J. Immunother. *35*, 689–701.
31. Tabata, Y., and Khurana Hershey, G.K. (2007). IL-13 receptor isoforms: breaking through the complexity. Curr. Allergy Asthma Rep. *7*, 338–345.
32. Uhlén, M., Fagerberg, L., Hallström, B.M., Lindskog, C., Oksvold, P., Mardinoglu, A., Sivertsson, Å., Kampf, C., Sjöstedt, E., Asplund, A., et al. (2015). Proteomics. Tissue-based map of the human proteome. Science *347*, 1260419.
33. Morrison, B.E., Marcondes, M.C., Nomura, D.K., Sanchez-Alavez, M., Sanchez-Gonzalez, A., Saar, I., Kim, K.S., Bartfai, T., Maher, P., Sugama, S., and Conti, B. (2012). Cutting edge: IL-13Rα1 expression in dopaminergic neurons contributes to their oxidative stress-mediated loss following chronic peripheral treatment with lipopolysaccharide. J. Immunol. *189*, 5498–5502.
34. Brown, C.E., Vishwanath, R.P., Aguilar, B., Starr, R., Najbauer, J., Aboody, K.S., and Jensen, M.C. (2007). Tumor-derived chemokine MCP-1/CCL2 is sufficient for mediating tumor tropism of adoptively transferred T cells. J. Immunol. *179*, 3332–3341.
35. Slaney, C.Y., Kershaw, M.H., and Darcy, P.K. (2014). Trafficking of T cells into tumors. Cancer Res. *74*, 7168–7174.
36. Croft, M. (2003). Costimulation of T cells by OX40, 4-1BB, and CD27. Cytokine Growth Factor Rev. *14*, 265–273.
37. Kong, S., Sengupta, S., Tyler, B., Bais, A.J., Ma, Q., Doucette, S., Zhou, J., Sahin, A., Carter, B.S., Brem, H., et al. (2012). Suppression of human glioma xenografts with second-generation IL13R-specific chimeric antigen receptor-modified T cells. Clin. Cancer Res. *18*, 5949–5960.
38. Keu, K.V., Witney, T.H., Yaghoubi, S., Rosenberg, J., Kurien, A., Magnusson, R., Williams, J., Habte, F., Wagner, J.R., Forman, S., et al. (2017). Reporter gene imaging of targeted T cell immunotherapy in recurrent glioma. Sci. Transl. Med. *9*, 10.1126/scitranslmed.aag2196.
39. Yaghoubi, S.S., Jensen, M.C., Satyamurthy, N., Budhiraja, S., Paik, D., Czernin, J., and Gambhir, S.S. (2009). Noninvasive detection of therapeutic cytolytic T cells with 18F-FHBG PET in a patient with glioma. Nat. Clin. Pract. Oncol. *6*, 53–58.
40. Jones, T.S., and Holland, E.C. (2012). Standard of care therapy for malignant glioma and its effect on tumor and stromal cells. Oncogene *31*, 1995–2006.
41. Riccardi, C., Cifone, M.G., and Migliorati, G. (1999). Glucocorticoid hormone-induced modulation of gene expression and regulation of T-cell death: role of GITR and GILZ, two dexamethasone-induced genes. Cell Death Differ. *6*, 1182–1189.
42. Dietrich, J., Rao, K., Pastorino, S., and Kesari, S. (2011). Corticosteroids in brain cancer patients: benefits and pitfalls. Expert Rev. Clin. Pharmacol. *4*, 233–242.
43. Banks, W.A., and Erickson, M.A. (2010). The blood-brain barrier and immune function and dysfunction. Neurobiol. Dis. *37*, 26–32.
44. Ahmed, N., Brawley, V., Hegde, M., Bielamowicz, K., Wakefield, A., Ghazi, A., Ashoori, A., Diouf, O., Gerken, C., Landi, D., et al. (2015). Autologous HER2 CMV bispecific CAR T cells are safe and demonstrate clinical benefit for glioblastoma in a Phase I trial. J. Immunother. Cancer *3* (*Suppl 2*), 011.
45. O'Rourke, D.M., Nasrallah, M., Morrissette, J.J., Melenhorst, J.J., Lacey, S.F., Mansfield, K., Martinez-Lage, M., Desai, A.S., Brem, S., Maloney, E., et al. (2016). Pilot study of T cells redirected to EGFRvIII with a chimeric antigen receptor in patients with $EGFRvIII^+$ glioblastoma. J. Clin. Oncol. *34* (*Suppl 15*), 2067.
46. Turtle, C.J., Hanafi, L.A., Berger, C., Gooley, T.A., Cherian, S., Hudecek, M., Sommermeyer, D., Melville, K., Pender, B., Budiarto, T.M., et al. (2016). CD19 CAR-T cells of defined $CD4^+$:$CD8^+$ composition in adult B cell ALL patients. J. Clin. Invest. *126*, 2123–2138.
47. Wekerle, H., Sun, D., Oropeza-Wekerle, R.L., and Meyermann, R. (1987). Immune reactivity in the nervous system: modulation of T-lymphocyte activation by glial cells. J. Exp. Biol. *132*, 43–57.
48. Adusumilli, P.S., Cherkassky, L., Villena-Vargas, J., Colovos, C., Servais, E., Plotkin, J., Jones, D.R., and Sadelain, M. (2014). Regional delivery of mesothelin-targeted CAR T cell therapy generates potent and long-lasting CD4-dependent tumor immunity. Sci. Transl. Med. *6*, 261ra151.
49. Katz, S.C., Point, G.R., Cunetta, M., Thorn, M., Guha, P., Espat, N.J., Boutros, C., Hanna, N., and Junghans, R.P. (2016). Regional CAR-T cell infusions for peritoneal carcinomatosis are superior to systemic delivery. Cancer Gene Ther. *23*, 142–148.
50. Pelloquin, F., Lamelin, J.P., and Lenoir, G.M. (1986). Human B lymphocytes immortalization by Epstein-Barr virus in the presence of cyclosporin A. In Vitro Cell. Dev. Biol. *22*, 689–694.
51. Jensen, M.C., Clarke, P., Tan, G., Wright, C., Chung-Chang, W., Clark, T.N., Zhang, F., Slovak, M.L., Wu, A.M., Forman, S.J., and Raubitschek, A. (2000). Human T lymphocyte genetic modification with naked DNA. Mol. Ther. *1*, 49–55.
52. Stastny, M.J., Brown, C.E., Ruel, C., and Jensen, M.C. (2007). Medulloblastomas expressing IL13Ralpha2 are targets for IL13-zetakine$^+$ cytolytic T cells. J. Pediatr. Hematol. Oncol. *29*, 669–677.